

Numerical Simulation on Hydrogen Behavior in a Small-Scale Cylindrical Container with Simulated Fuel Debris

K. Takase*, Y. Hiraki*, G. Takase*, Y. Tanaka* and Y. Suzuki*
Corresponding author: takase@vos.nagaokaut.ac.jp

* Nagaoka University of Technology, Japan

Abstract: Fuel debris which is removed from the Fukushima Dai-ichi Nuclear Power Plant is packed to the radioactive waste long-term storage containers. When the fuel debris includes water, hydrogen and oxygen are generated by decomposition of water by radiation from the fuel debris. Since hydrogen is flammable gas, it has a risk of combustion and explosion. Therefore, it is important to clarify the hydrogen behavior in the radioactive waste long-term storage container under the conditions that the fuel debris containing water is accumulated. As for former studies of hydrogen behavior in the sealed container, experimental and analytical studies on hydrogen behavior under the various conditions of the fuel debris have not been conducted sufficiently. Then, the influence of hydrogen flow rate, temperature, porosity, etc. upon the hydrogen behavior was predicted numerically. As a result of this, the controlling factors which define the hydrogen behavior in the radioactive waste long-term storage container were clarified.

Keywords: Numerical Simulations, Hydrogen Behavior, Cylindrical Container, Fuel Debris, Controlling Factors.

1 Introduction

Fuel debris which is removed from the Fukushima Dai-ichi Nuclear Power Plant (1F) is packed to the inside of a radioactive waste long-term storage container. When the fuel debris includes water, hydrogen and oxygen are generated by decomposition of water by radiation from the fuel debris. Since hydrogen is flammable gas, it has a risk of combustion or explosion. Therefore, it is important to clarify the hydrogen behavior in the radioactive waste long-term storage container under the conditions that the fuel debris containing water is accumulated. Moreover the bulk density of the fuel debris is not constant and the arrangement of that in the container is not uniform. That is, it is considered that the fuel debris accumulated in the container has arbitrary distributions in the vertical and horizontal directions on the bulk density and the arrangement depending on the packing condition of the fuel debris into the container. However, it is not easy to clarify hydrogen behavior in the storage container experimentally in terms of time and cost. Therefore, we conducted numerical simulations.

As for studies of hydrogen behavior in the sealed container, Inoue, et al. [1] evaluated experimentally hydrogen diffusion characteristics using the Hallway model. Hoyes and Ivings [2] performed CFD modelling of hydrogen stratification in enclosures. Visser, et al. [3] predicted numerically hydrogen distributions in a containment vessel. However, experimental and analytical

studies on hydrogen behavior to various packing conditions of the fuel debris have not been found.

Then, the influence of the bulk density, arrangement, etc. upon the convection behavior of hydrogen was investigated numerically. The present study shows the predicted results on convection behavior of hydrogen in a simply simulated radioactive waste long-term storage container. Moreover, controlling factors which define the convection behavior of hydrogen are described.

2 Numerical Analysis

2.1 Governing Equations

For the analysis, The ANSYS FLUENT was used. The governing equations on thermal-hydraulics of the multi-component gases considering compressibility are as follows.

- Mass conservation equation

$$\frac{\partial p}{\partial t} + \frac{\partial}{\partial x_j}(\rho u_j) = 0$$

- Momentum conservation equation

$$\frac{\partial}{\partial t}(\rho u_i) + \frac{\partial}{\partial x_j}(\rho u_i u_j) = -\frac{\partial p}{\partial x_i} + \frac{\partial}{\partial x_j} \left[\mu \left(\frac{\partial u_i}{\partial x_j} + \frac{\partial u_j}{\partial x_i} \right) \right] + \rho g_i$$

- Energy equation

$$\frac{\partial}{\partial t}(\rho h) + \frac{\partial}{\partial x_j}(\rho h u_j) = \frac{\partial p}{\partial t} + u_j \frac{\partial p}{\partial x_j} + \frac{\partial}{\partial x_j} \left(\lambda \frac{\partial T}{\partial x_j} \right) + \frac{\partial}{\partial x_j} \left(\rho \sum_s h_s D_s \frac{\partial Y_s}{\partial x_j} \right) + Q$$

- Mass conservation equation of species

$$\frac{\partial}{\partial t}(\rho Y_s) + \frac{\partial}{\partial x_j}(\rho Y_s u_j) = \frac{\partial}{\partial x_j} \left(\rho D_s \frac{\partial Y_s}{\partial x_j} \right)$$

- Equation of state

$$p_s = \rho_s \frac{R_0}{M_s} T$$

The density ρ , pressure p , enthalpy h and mass fraction Y_s and in the above basic equations are defined as follows.

$$p = \sum_s p_s$$

$$h = \sum_s Y_s h_s$$

$$Y_s = \frac{\rho_s}{\rho}$$

2.2 Porous Model

In the porous media, the empirically determined flow resistance is used to the region defined as “porous” [4]. The porous media is modeled by the addition of a momentum source term to the standard fluid flow equations. The source term can be seen in the following equation is composed of two parts; a viscous loss term and an inertial loss term.

$$S_i = - \left(\sum_{j=1}^3 D_{ij} \mu v_j + \sum_{j=1}^3 C_{ij} \frac{1}{2} \rho |v| v_j \right)$$

Where, S_i is the source term for the i-th (x, y, or z) momentum equation, $|v|$ is the magnitude of the velocity, and D and C are prescribed matrices.

In the present study the porous media is assumed as homogeneous and the following equation is derived.

$$S_i = - \left(\frac{\mu}{\alpha} v_i + \sum_{j=1}^3 C_2 \frac{1}{2} \rho |v| v_j \right)$$

Where, α is the permeability and C_2 is the inertial resistance factor. From the assumption of packed beds, those values are shown as

$$\alpha = \frac{D_p^2}{150} \frac{\varepsilon^3}{(1 - \varepsilon)^2}$$

$$C_2 = \frac{3.5 (1 - \varepsilon)}{D_p} \frac{1}{\varepsilon^3}$$

The scheme of solution method uses the SIMPLE. In order to analyze transport behavior of two component gases between air and hydrogen, the mixture model was chosen. The mixture model is given to the fluid in the container initially.

3 Analytical Conditions

3.1 Computational Grid

Figure 1 shows the computational grid used in the present calculation. It was set to 45×90 cells, and adopted a non-uniform mesh division which makes the wall side finer. The radioactive waste storage container was simulated by a sealed two-dimensional rectangular container with dimensions of 900 mm in height and 450 mm in width. The region where the fuel debris is filled was assumed as porous media and the porous model was applied. In the calculation, the packed bed model which is one of porous model was used. In the packed bed model, it is expressed by inertial resistance and viscous resistance which can be obtained by both equations of α and C_2 . The resistances of those equations are determined by the porosity and the representative particle diameter. The decay heat is simulated by giving heat transfer rate to the porous region. The generation of hydrogen is simulated by flowing hydrogen with a constant velocity from the nozzle which is installed at the bottom of the container.

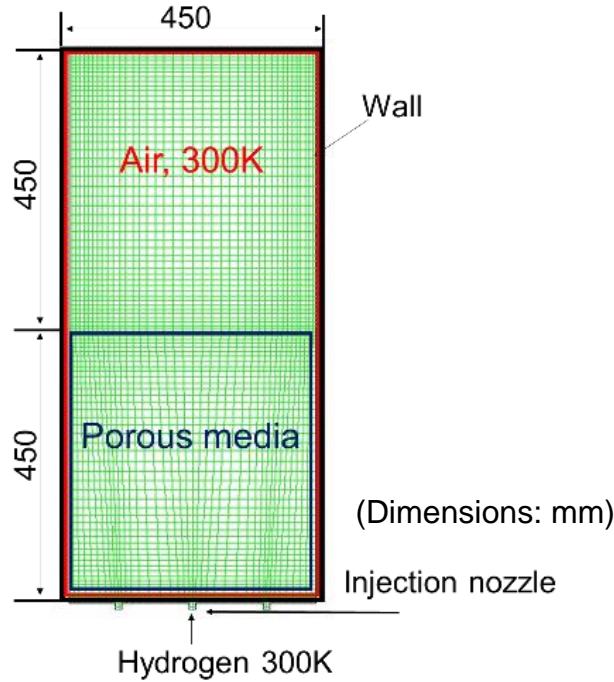


Fig. 1 Computational grid

The dimensions of the container are the same as the experimental apparatus. Figure 2 shows an appearance of an experimental apparatus which consists of a simulated container and a controller and also the outline of the internal structure. Here the simulated decay heat heaters can be seen by four red bars and the simulated fuel debris is installed to the inside of the lower half of the container. The hydrogen gas is discharged from the outside of the container into the inside. Here the passive autocatalytic recombiner (PAR) is installed into the inside in order to reduce the hydrogen concentration by combining hydrogen and oxygen based on chemical reaction of hydrogen and PAR.

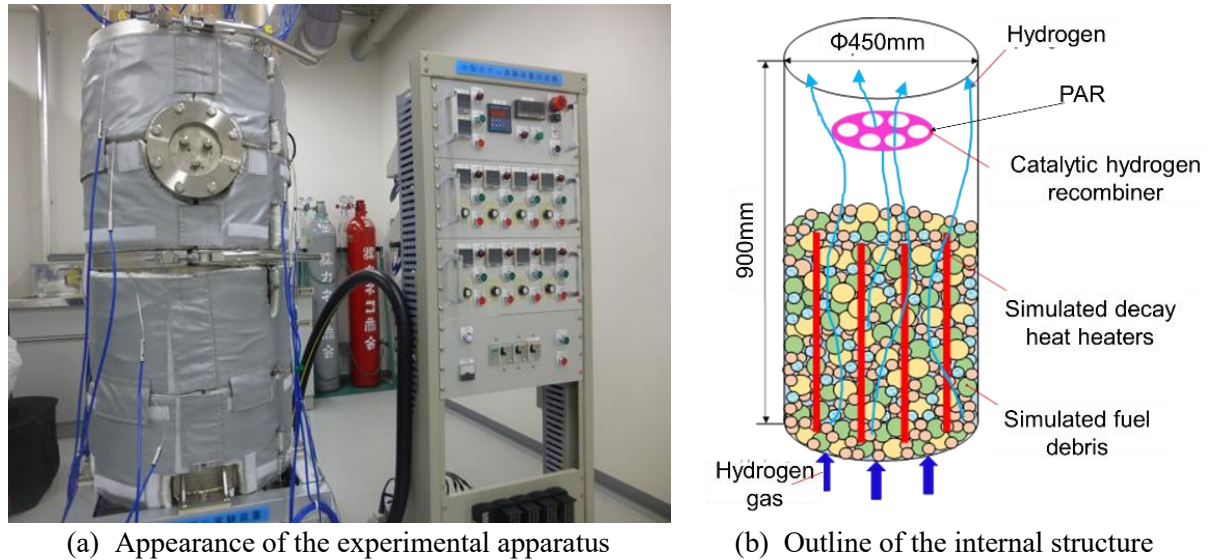


Fig. 2 Overview of an experimental apparatus

As initial conditions, the mass fraction of hydrogen is set to 0 and that of air becomes 1. That is, the inside of the container is initially occupied with only air. The hydrogen is discharged with time at the constant velocity. Moreover, when the heated condition is calculated, the heat transfer rate is given to the region of porous media as the decay heat. The lower half of the container is set to be porous, and hydrogen is flowed from the one or three nozzles at the bottom of the container.

3.2 Calculation Parameters

Table.1 shows the controlling factors that seem to influence to the hydrogen behavior. Controlling factor is considered to be the production rate of hydrogen, the generation rate of hydrogen, the amount of decay heat and the bulk density of fuel debris. In order to use these factors for the present calculations, the inlet velocity of hydrogen, the heat transfer rate and the porosity of the porous media are used as the parameters.

Table.1 Estimated controlling factors

<i>Controlling factors</i>	<i>Analysis time conditions</i>	<i>Estimated parameters</i>
Hydrogen generation rate	Inlet velocity&Inflow time	H ₂ mole fraction
Decay heat	Heat transfer rate is given as a source term	Temperature
Bulk density of the fuel debris	Packed bed model is defined by porosity and particle diameter	Friction loss

In the present calculations, the hydrogen generation rate was estimated from the predicted amount of decay heat. The amount of decay heat was calculated using the TODRES equation [5-7] as shown by,

$$\frac{P(t)}{P_0} = 0.066[t^{-0.2} - (t_s + t)^{-0.2}]$$

Where P is the decay heat, P_0 is the thermal output during normal operation of the reactor, t is the elapsed time since reactor shutdown and t_s is the time after the fuel rod is started to be used. P_0 is given 1380 MW from the data of 1F [7-8]. t_s is given 1.74 years from reference [7],[9]. The calculation result of $P(t)/P_0$ is shown in Fig. 3. The horizontal axis is the elapsed time after the reactor shutdown and the vertical axis is the ratio of the decay heat and the thermal output during normal operation. Subsequently, on the assumption that fuel debris is packed in the entire container, the amount of decay heat is calculated using the volume of the container. The derived equation is,

$$P' = \frac{P \times V}{9.924}$$

Where P' indicates the decay heat of the fuel debris packed in the container, V is the volume of the container and the volume of UO_2 used to all the fuel rods in 1F becomes 9.924 (m^3). The calculation result is shown in Fig.4. Here the horizontal axis indicates the elapsed time from the reactor shutdown of the F1 and the vertical axis shows the amount of decay heat.

In addition, the hydrogen generation rate was estimated from the amount of decay heat and the generation rate (G rate) of hydrogen. Here the rate of 4.7×10^{-8} mol/J was given as the G rate of hydrogen from reference [10] and [11]. The calculation results are shown in Fig.5. The horizontal axis shows the amount of decay heat and the vertical axis represents the G rate of hydrogen.

As calculation parameters, three kinds of heat transfer rate, 31,000 W, 7600 W and 830 W, were used. Each heat transfer rate corresponds to the decay heat of UO_2 after 1 month, 1 year or 10 years from the Fukushima accident, respectively. Similarly, as for the hydrogen flow rate discharged into the bottom of the container, three kinds of the inlet velocities of hydrogen, 001, 0.1 and 0.4 m/s, were used as the calculation parameter and each velocity corresponds to the decay heat of UO_2 after 1 month, 1 year or 10 years from the Fukushima accident, respectively. Each velocity was calculated from the inlet pipe diameter of 10 mm and the hydrogen generation rate. For setting of porosity and representative particle size, the particle diameter, d , was fixed to 10 mm and the porosity, ε , was set to 0.2 (i.e., condition with many substance), 0.5 (condition of 50% gas and 50% solid), and 0.8 (condition with many space).

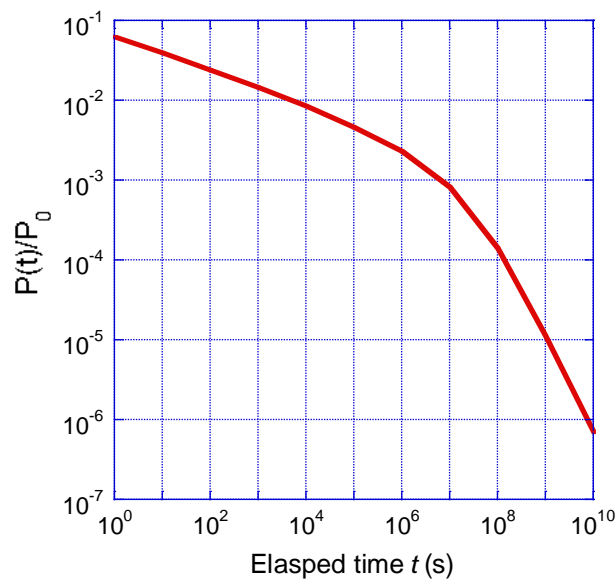


Fig. 3 Change in $P(t)/P_0$ with respect to elapsed time

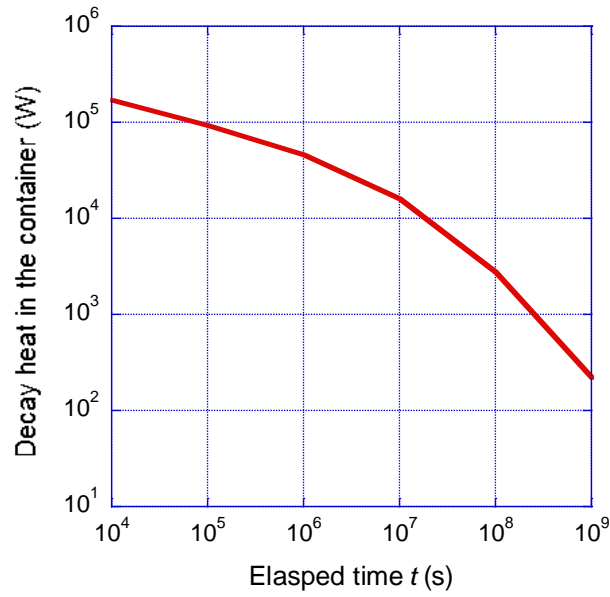


Fig. 4 Change in decay heat in the container with respect to elapsed time

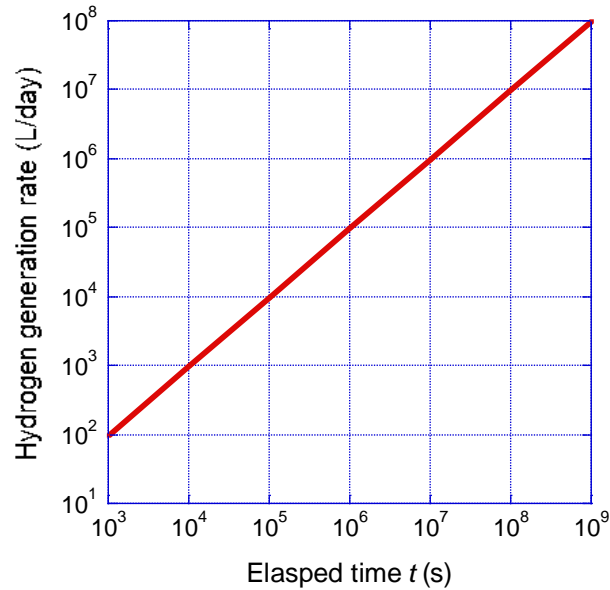


Fig. 5 Change in hydrogen generation rate with respect to elapsed time

4 Results and Discussion

The preliminary calculations were performed under the unsteady-state condition. The calculation time was 10 s, and the time step, ΔT , was 0.1 s. Figure 6 shows the predicted hydrogen mole concentration distributions at the inlet velocities of 0.1 m/s and 0.4 m/s. As a difference of both predictions, the result when the inlet velocity is 0.4 m/s shows that diffusion of hydrogen is observed in the upper region of the container and the concentration is higher than that when it is 0.1 m/s.

The relationship between the inlet velocity and mole concentration is shown in Fig. 7. The horizontal axis indicates the inlet velocity and the vertical axis represents the maximum mole concentrations of hydrogen in the porous and non-porous regions. When the inlet velocity is lower than 0.02 m/s, the maximum mole concentrations of hydrogen at both regions are almost close to 0. In case of the porous region, the maximum mole concentrations of hydrogen increases very quick after

0.02 m/s and becomes approximately 0.04 after the inlet velocity is 0.07 m/s. On the other hand, in case of the non-porous region, the maximum mole concentrations of hydrogen gradually increases with the inlet velocity and reaches to around 4 at the inlet velocity of 1 m/s.

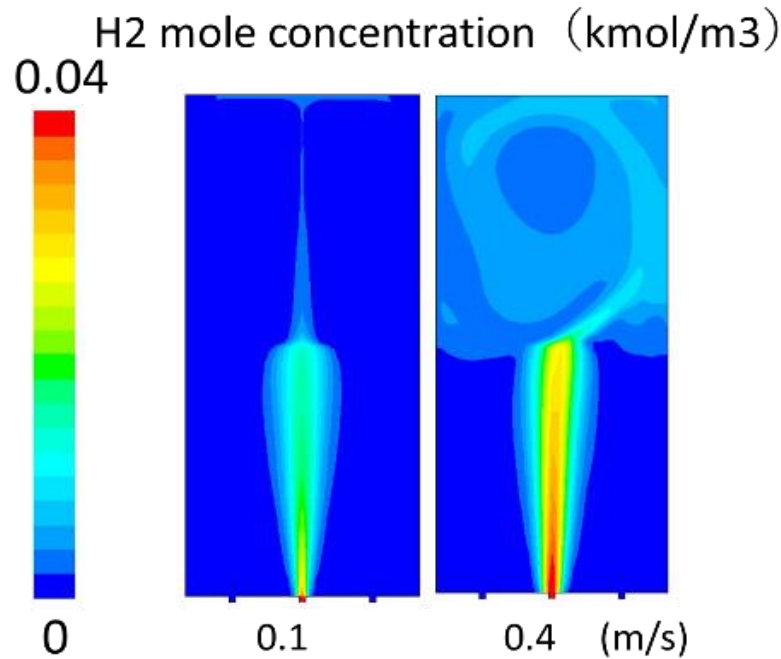


Fig. 6 Mole concentrations of hydrogen when hydrogen the inlet velocities are 0.1 and 0.4 m/s

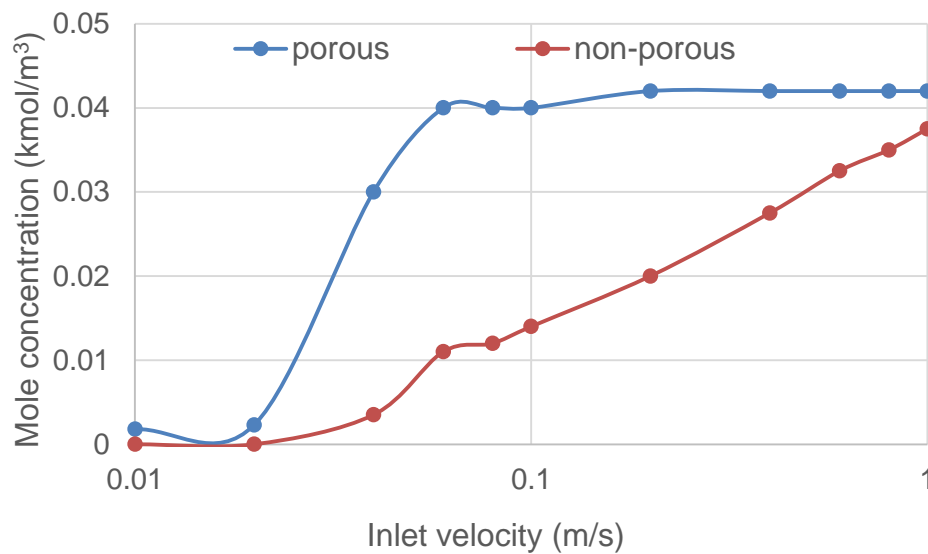


Fig. 7 Maximum mole concentrations of hydrogen at porous and non-porous regions

Calculations up to 300 s were performed to check the effect on heat transfer rate at the porous region. Figure 8 shows the fluid temperature distributions when the heat transfer rates are 7,600 and 31,000 W. Here, calculation conditions are: the inlet velocity of hydrogen is 0.1 m/s, the porosity of the porous region is 0.5 and the time from the start of calculation is 10 s. The fluid temperature increases with the heat transfer rate. In case of Fig. 8, the fluid temperature difference is 4 K for 7600 W and 8 K for 31000 W.

The relationship between the heat transfer rate and fluid temperature is shown in Fig. 9. The horizontal axis is the heat transfer rate and the vertical axis is the fluid temperature difference ΔT at both center positions in the porous region and the non-porous region. From the predicted results, it was confirmed that the temperature increase at both regions shows logarithmically.

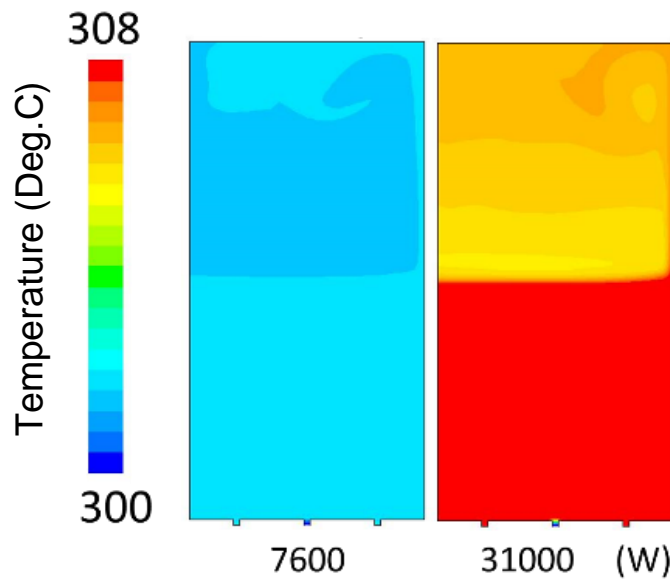


Fig. 8 Temperature distributions at different heat transfer rates

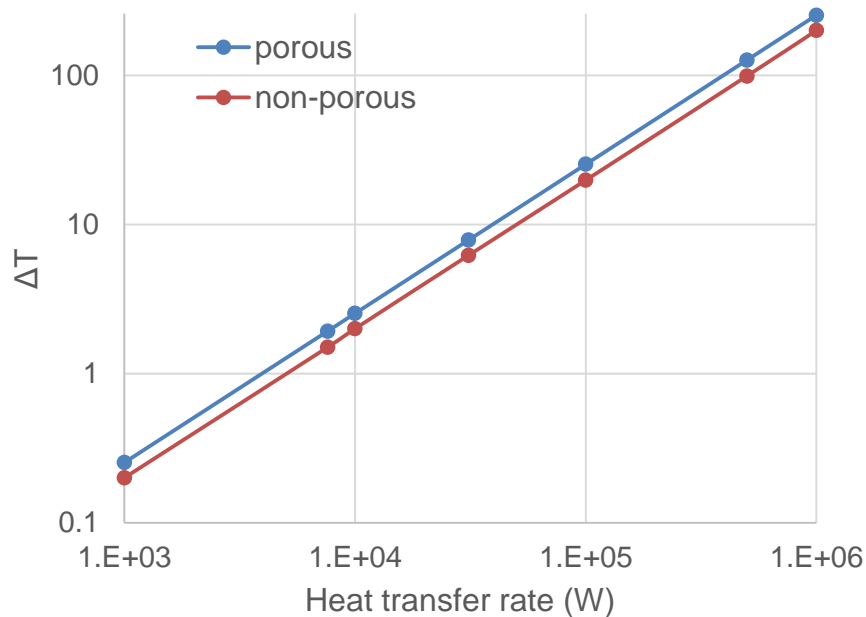


Fig. 9 Relationship between ΔT and heat transfer rate

As can be seen in Fig. 10, calculations up to 10 s were performed to check the effect on porosity. The calculation conditions are that the inlet velocity is 0.1 m/s; heating transfer rate at the porous region When the porosity is 0.8, is 7600 W; and two kinds of porosities, 0.5 and 0.8, are given to the porous region as a calculation parameter. The difference in the porosity used in the packed layer model is represented by the difference between inertial resistance and viscous resistance. In this calculation, the particle size was fixed at 10 mm in order to confirm the effect of porosity. The fluid velocity distributions when the porosity is 0.4 and 0.8 are shown in Fig. 10. When the porosity is 0.8, a fluid

flow quickly reaches the upper region (i.e., non-porous region) in the container in comparison with the condition that the porosity is 0.4, and a circulation flow is confirmed in the upper region.

The relationship between the inertial resistance derived from the equation of C_2 and the porosity is shown in Fig. 11. Here, the horizontal axis shows porosity and the vertical axis represents the inertial resistance. When the porosity is higher, the inertial resistance becomes higher and the particle diameter is smaller. The difference in the inertial resistance between the particle diameter of 10 mm and 100 mm was 10^2 .

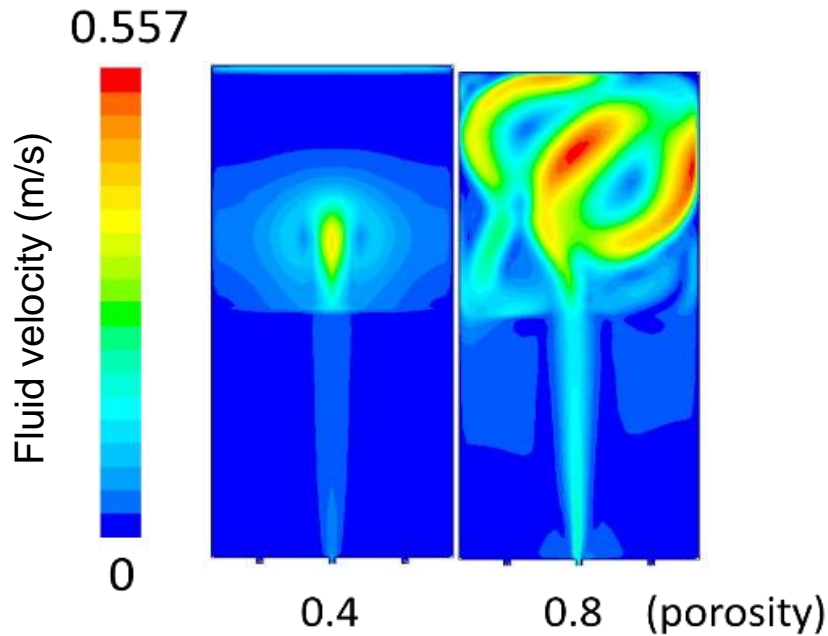


Fig. 10 Fluid velocity distributions at different porosities

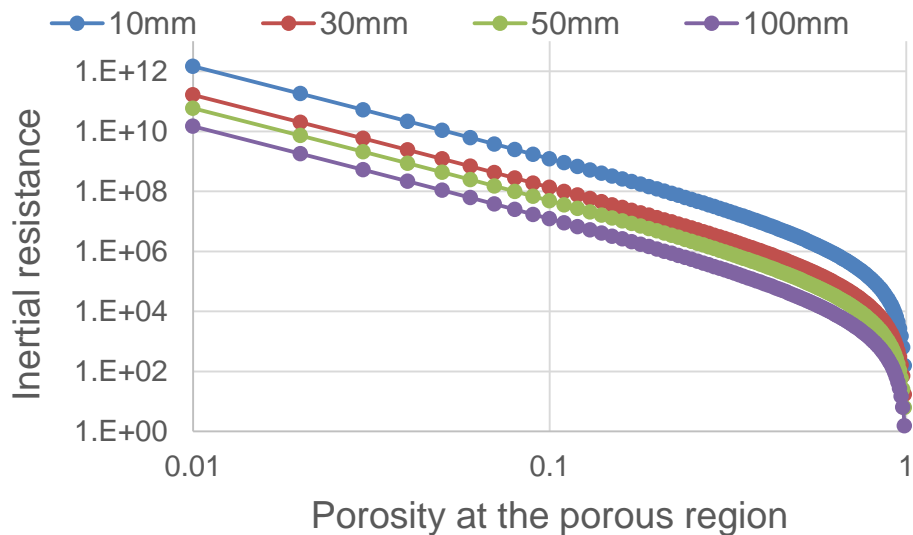


Fig. 11 Relationship between inertial resistance and porosity at the porous region

As an example, predicted density and temperature distributions are shown in Fig.12. Hydrogen does not mix with air in the porous media and rises straight up as can be seen in blue three lines. Air and hydrogen are mixed in the upper region of the porous media and a large recirculation flow is generated. In the temperature distribution, since the porous media acts as a large heat sink, the rise in

the fluid temperature in this region is remarkable. The maximum fluid temperature is 500K and appears in the porous media.

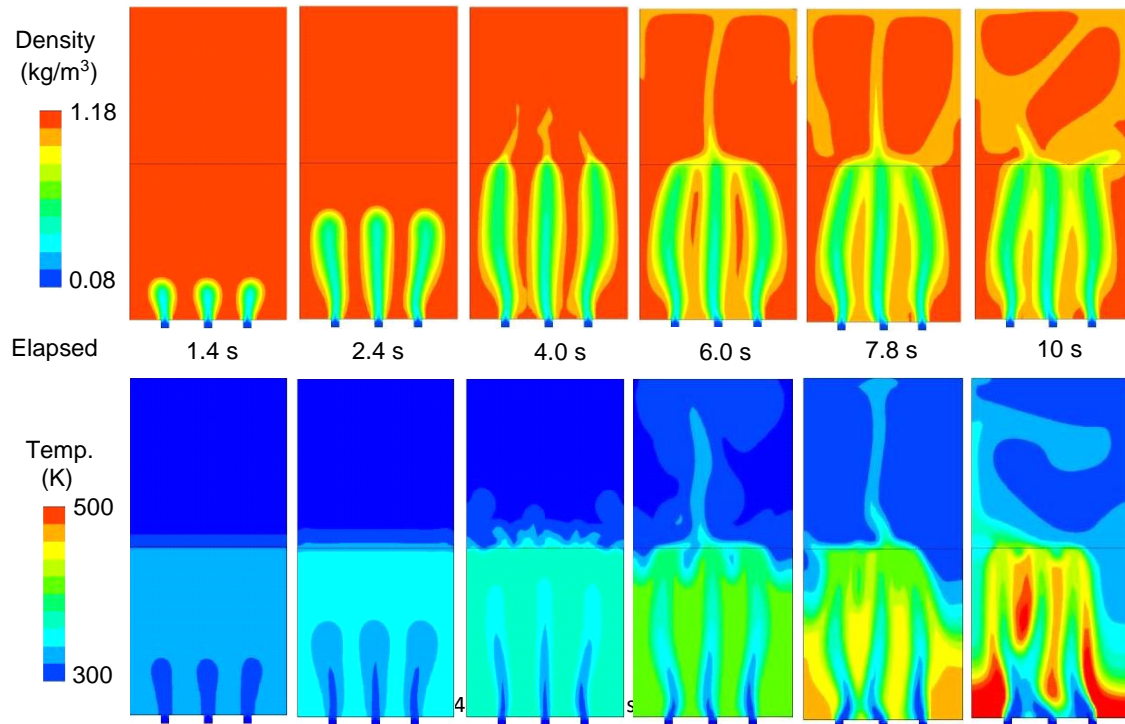


Fig. 12 Predicted density and temperature distributions with time under the heated condition

5 Conclusions

The numerical simulations were conducted to investigate the hydrogen behavior in the radioactive waste long-term storage container associated with the decommissioning of 1F and the controlling factors which defines the hydrogen behavior were considered numerically, and each effect of the hydrogen generation rate, decay heat or bulk density of the fuel debris on the hydrogen behavior was clarified. As a result, the following conclusions were derived:

- 1) As for the effect of the hydrogen generation rate, the mixing of hydrogen and air is enhanced with increasing the inlet velocity of hydrogen;
- 2) As for the effect of the decay heat rate, the fluid temperature increases with the heat transfer rate, and as a result, the hydrogen velocity is accelerated because the buoyancy effect increases; and
- 3) As for the bulk density of the fuel debris, the hydrogen flow receives strongly the effect of porosity in the porous region. When the porosity is small, since the pressure loss in the porous media increases, the passing time in the porous region of hydrogen is long.

As a future plan, chemical reaction simulations will be performed to clarify performance of the passive autocatalyst recombiner against the generation of hydrogen.

Nomenclature

- C_2 Inertial resistance factor [1/m]
 D_p Mean particle diameter [m]
 D_s Effective diffusion coefficient of chemical species s [m^2/s]
 g Gravity [m/s^2]
 h Enthalpy [J/kg]
 h_s Enthalpy of chemical species s [J/kg]

M_s	Molecular weight of chemical species s [kg/mol]
P	Decay heat [W]
P_0	Thermal output during normal operation of the reactor [W]
P'	Decay heat rate in the volume of the container [W]
p	Pressure [Pa]
p_s	Partial pressure of chemical species s [Pa]
Q	Calorific value [W/m ³]
R_0	Universal gas constant (= 8.314) [J/mol/K]
T	Temperature [K]
t	Time [s]
t_s	Used time of fuel rod [s]
u	Velocity [m/s]
V	Volume [m ³]
x	Coordinates [m]
Y_s	Mass fraction of chemical species s [-]
α	Permeability [m ²]
ϵ	Porosity [-]
λ	Heat conduction coefficient [W/m/K]
μ	Viscosity [Pa·s]
ν	Kinetic viscosity [m ² /s]
ρ	Density [kg/m ³]
ρ_s	Density of chemical species s [kg/m ³]
Subscripts	
i	x direction lattice index
j	y direction lattice index

Acknowledgments

A part of this study is the result of “Research and development on technology for reducing the concentration of flammable gases generated in waste long-term storage containers” carried out under the Center of World Intelligence Project for Nuclear S&T and Human Resource Development by the Ministry of Education, Culture, Sports, Science and Technology of Japan.

References

- [1] M. Inoue, H. Tsukikawa, H. Kanayama, K. Matsuura, Experimental Study on Leaking Hydrogen Dispersion in a Partially Open Space, Hydrogen energy system, Vol.33, No.4, pp.32-43, (2008).
- [2] J. R. Hoyes, M. J. Ivings, CFD modelling of hydrogen stratification in enclosures: Model validation and application to PAR performance, Nuclear Engineering and Design 310, pp.142-153, (2016).
- [3] D. C. Visser, M. Houkema, N. B. Siccama, E. M.J . Komen, Validation of a FLUENT CFD model for hydrogen distribution in a containment, Nuclear Engineering and Design 245, pp.161-171, (2012).
- [4] ANSYS FLUENT Theory Guide, (2015), (in Japanese)
- [5] N. E. Todreas and M. S. Kazimi, Nuclear Systems I, Thermal Hydraulic Fundamentals, Hemisphere Publishing Corporation, 1990, ISBN 0-89116-935-0 v.1.
- [6] McMaster Nuclear Reactor, McMaster University, “Decay Heat Estimates for MNR”, Technical Report 1998-03 <http://www.nuceng.ca/papers/decayhe1b.pdf>

- [7] K. Mariyama, Tohoku University Institute of Fluid Sciences, Estimation of the amount of water required when the interior of the nuclear reactor is heated only by decay heat, Heat-Transfer Control Lab. Report No. 1, Ver. 4 (HTC Rep. 1.4 2011/04/13).
- [8] TEPCO, "Outline of Fukushima Daiichi Nuclear Power Station facility",
http://www.tepco.co.jp/nu/fukushima-np/outline_f1/index-j.html
- [9] TEPCO, "Periodical Inspection Result", http://www.tepco.co.jp/nu/f1np/data_lib/pdfdata/bk1011-j.pdf.
- [10] T. Kumagai, Japan Atomic Energy Agency, Radiolysis of water and treatment of radioactive contaminated water with zeolite, The 46th Japan Atomic Energy Society Award Encouragement Prize (No. 4609).
- [11] G. V. Buxton, The radiation chemistry of liquid water: principles and applications. In: Mozumder, A., Hatano, Y. (Eds.), Charged Particle and Photon Interactions with Matter. Marcel Dekker, Inc., New York. pp.331-363, (2004).